Research Article……..

International Journal of Agricultural Invention

(online available at www.agriinventionjournal.com)

***International Journal of Agricultural Invention* 8(1): 87-106: June, 2023**

ISSN: 2456 – 1797 (P)

Implementing a gaseous fuel mixing system to use in a 30 kW burner and survey on laminar flame speed

***Mohammad Ghoreishi[1], Paolo Venturini[2], Carmine Mongiello[3], Vinod Kumar Sharma[4], Joginder Singh[5]**

[1]Astronautical, Electrical and Energy Engineering, Sapienza University of Rome, Via Eudossiana 18, Rome, Italy
[2]Department of Mechanical and Aerospace Engineering, Sapienza University of Rome, Via Eudossiana, Rome, Italy
[3]Research Centre Portici, Laboratory of Thermochemical Processes for Wastes and Biomass Valorization, Division of Bioenergy, Energy Technologies and Renewable Sources Department, Italian National Agency for New Technologies, ENEA, Portici, Italy
[4]Research Centre Trisaia, Division of Bioenergy, Biorefinery and Green Chemistry, Italian National Agency for New Technologies, ENEA, Rotondella (MT), Italy
[5]Department of Horticulture, J. V. College, Baraut, UP, India
***Corresponding email**: *mohammad.ghoreishi@uniroma1.it*

ARTICLE INFO

Research Article
Received on April 15, 2023
Revised on April 27, 2023
Accepted on May 09, 2023
Published on June 05, 2023

Article Authors
Mohammad Ghoreishi,
Paolo Venturini,
Carmine Mongiello,
Vinod Kumar Sharma,
Joginder Singh

Corresponding Author Email
mohammad.ghoreishi@uniroma1.it

PUBLICATION INFO
International Journal of Agricultural Invention (IJAI)
RNI: UPENG/2016/70091
ISSN: 2456-1797 (P)
Vol.: 8, **Issue:** 1, **Pages:** 87-106
Journal Homepage URL
http://agriinventionjournal.com/
DOI: 10.46492/IJAI/2023.8.1.13

ABSTRACT

This paper contains the optimal design of a natural gas and hydrogen supply and mixing station for the combustor test facility and the laminar flame speed and burning velocity investigation. Our first goal is a piping/process and instrumentation drawing (P&ID) and Process Flow Diagram (PFD) which include the type and connection of different gases, flow rates, tube sizing, and implemented equipment in this design and it is divided into two parts. One part is provided by the Catholic University of Leuven after considering Health and Safety and Environment (HSE) actions. The second and more critical part is provided by external suppliers, and it consists of two design phases, namely the gas mixing panel and the gas splitting panel. External companies that design, produce, and supply the panels are divided into two groups, which provide mass flow controller/meter and gas mixing/splitting panel respectively in order to provide the optimal and optimized mixing system. In addition, survey results also revealed that laminar burning velocity (LBV) in hydrogen-air mixtures is almost six times greater than methane-air combustion velocity. In addition, a significant increase in the laminar flame speed of the CH_4-CO_2-O_2 mixture has been recorded as the oxygen concentration increased from 25% to 35%, confirming that hydrogen and oxygen positively impact the laminar flame speed in different percentages. Although lots of experimental research has been done on hydrogen-enriched oxy-combustion, this topic remains interesting for researchers to improve combustion efficiency. Finally, an optimal and cost-effective design of a gaseous fuel mixing system is the outcome of this work that will be used for performing measurement and test activities in the future.

KEYWORDS

Combustion, Gaseous Fuel System, Industrial Burner, Greenhouse Gas Emission, Laminar Flame Speed

HOW TO CITE THIS ARTICLE

Ghoreishi, M., Venturini, P., Mongiello, C., Sharma, V. K., Singh, J. (2023) Implementing a gaseous fuel mixing system to use in a 30 kW burner and survey on laminar flame speed, *International Journal of Agricultural Invention,* 8(1): 87-106. DOI: 10.46492/IJAI/2023.8.1.13

Recent economic developments have focused on reducing greenhouse gas emissions and limiting the effects of the climate change. Governments have started to produce renewable energies that mitigate emissions, but they are weather-dependent and intermittency-prone, requiring continuous supply and CO_2 emissions from fossil fuel power plants have a significant role in global warming and climate change (Kharel and Shabani, 2018). To reduce CO_2 emissions, improvements in combustion efficiency and conversion to natural gas might reduce carbon dioxide emissions.

An oxy-combustion technique is used to extract CO_2 from flue gas, removing nitrogen dilution from the combustor input and producing a flue gas primarily constituted of CO_2 (Thambimithu *et al*., 1998, Palmer *et al*., 1999). Conventional diesel engines used a variety of gaseous fuels, including coal gas, sewage gas, or methane (Karim, 1987). The gaseous fuel mixing system is desirable in burner technology and gas turbine applications due to its compact combustion and low NO_x emissions. A chemical reaction in which fuel is oxidized and a considerable amount of energy is known as combustion. Thermal conversion systems will play a critical part in the chain of energy supply (D'Alessio and Moccia, 2013). Connecting green hydrogen to the natural gas grid helps to reduce greenhouse gas emissions and makes it easier for the market to absorb hydrogen (Al-Alousi *et al*., 1996). Hydrogen combined with compressed natural gas (HCNG) has been explored for internal combustion engine combustion for the past two decades (Rosseel and Sierens, 2000). Mixing a specific proportion of hydrogen with natural gas has been demonstrated in numerous studies to enhance combustion heat efficiency and reduce pollution emissions (Mehra *et al*., 2020 and Penev *et al*. 2013). Burners for hydrogen-natural gas combinations in residential applications are being improved in terms of stability and reliability while emitting acceptable levels of NO_x and total hydrocarbons (THCs).

Hydrogen has a high burning speed and lower minimum igniting energy and according to the literature assessment report of life cycle and socio-economic assessment aspects, adding hydrogen to natural gas has the following advantages: a considerable decrease in greenhouse gas emissions, possible advantages of selective hydrogen extraction, possible advantages of recovering the air quality, and possible "greening" advantages of directly using the hydrogen/natural gas mixture in current applications for heat and electricity production (Mortimer, 2009). Witkowski *et al.* (2018) and Ogden *et al.* (2018) argue that mixing hydrogen in natural gas pipelines needs to consider a variety of issues, including market, economy, technology, and pipeline network architecture. Industrial burner and furnace development testing can save money in terms of development expenses and time for hardware validation trials. This study used an experimental natural gas swirl burner designed by International Flame Research Foundation (IFRF) based on the Near Field Aerodynamics (NFA) project (Hagiwara *et al*., 1984). The chamber for combustion is equipped with continuous and inflame measuring devices to monitor the flame behavior and investigate it for a limited number of configurations (Driscoll *et al*., 1993).

There is a lot of previous research on combustion efficiency, but the goal of this paper is to design an optimal and cost-effective gaseous fuel mixing system that will be used for research activities in the future. In fact, this paper investigates the optimal design of a gas supply and mixing station for the combustor test facility, which will be able to burn natural gas with the addition of hydrogen and air with the addition of O_2/ CO_2 (oxy-combustion) based on the oxygen fraction. The rest of the paper is structured as follows: the literature study is described in section 2, followed by the methodology and laminar burning velocity survey described in section 3. The main result and design of the gaseous fuel mixing system is the outcome of section 4 which consists of two sections. The first section contains P&ID, fuel/ air supply flow rate, and tube sizing calculations and the second section includes equipment selection and suppliers. Finally, section 5 provides the main conclusions and recommendations for future work.

Fig 1. 30 kW IFRF research burner

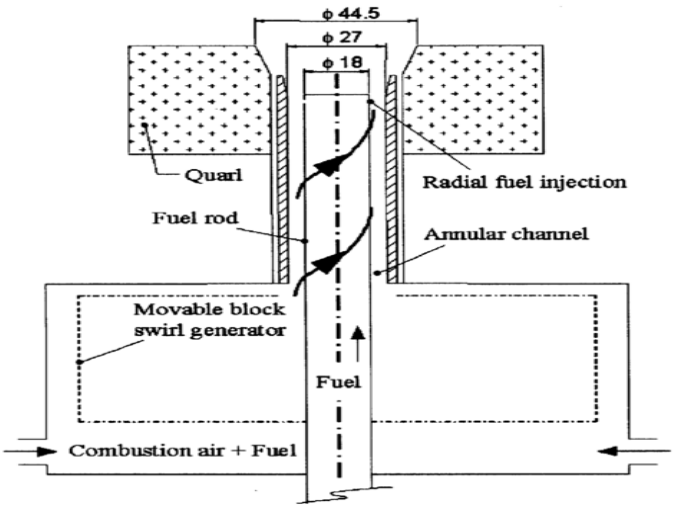

Fig 2. 30 kW IFRF swirl burner schematic

Literature Study

Natural Gas and Hydrogen

The World Energy Outlook (WEO) predicts that natural gas will play a large role in energy production and demand in the future due to its environmental benefits and adaptability compared to other combustible fuels (https://www.iea.org/weo2018/scenarios/2018). Natural gas is mostly composed of methane, with traces of ethane, propane, butane, nitrogen, carbon dioxide, and helium. According to (Perry, 1963), natural gas has an average gross heating value of 45,843 (KJ/kg), ranging from 42,697 to 47,192 (KJ/kg), and is the least polluting fossil fuel, emitting the least amount of CO_2 per energy unit and overall expenditure has been gradually increasing by 1.6% in recent years. It is critical to understand its combustion properties to meet energy efficiency and environmental goals and its core chemistry process has a considerable impact on the combustion of heavier hydrocarbons than methane (Dryer *et al.*, 1984). Instead, hydrogen can be added to hydrocarbon fuels to reduce pollution in cities and bring it into the energy supply infrastructure. Alternative energy research has recently gained importance, particularly for future global energy stability.

Hydrogen has numerous advantages, including renewable energy, significant specific energy per mass, safe transportation in pipelines, the ability to be generated from fossil fuels, and the ability to be used as a chemical raw material. There are few numerical and experimental investigations on hydrogen combustion in burners (Dincer *et al*., 2005). Choudhuri and Gollahalli (2003) investigated the combustion characteristics of hydrogen and mixed hydrogen with hydrocarbon compound fuel in a small vertically square cross-sectional combustion chamber. Hydrogen is classified as gray, blue, or green depending on how it is produced. At standard conditions, one cubic meter of hydrogen weighs 0.082 kg or 12% of the weight of natural gas. It is possible to reduce CO_2 emissions by mixing hydrogen and natural gas in the fuel stream but achieving a 50% decrease in CO_2 emissions takes roughly 75% H_2 by volume due to the difference in energy content. Hydrogen has lower minimum ignition energy than methane and a broader range of flammability limitations. Hydrogen is generally used with other fuels in industrial applications but regular burners, on the other hand, are not designed to burn hydrogen and natural gas mixtures in houses for safety concerns. Table 1 shows the combustion characteristics of hydrogen and methane.

Table 1. Combustion properties of hydrogen and methane

Property	Hydrogen	Methane
Density of gas at NTP[a] ($kg.m^{-3}$)	0.0838	0.6512
Heat of combustion[b](low) ($MJ.m^{-3}$)	10.78	39.72
Heat of combustion[b]($high$) ($MJ.m^{-3}$)	12.75	35.80
Flammability range (limits) in air[c](%)	4.1 - 75	5.3 - 15
Stoichiometric composition in air[c] (%)	29.53	9.48
Minimum ignition energy (mJ)	0.02	0.29
Minimum self-ignition temperature[d] (K)	858	813
Adiabatic flame temperature in air (K)	2318	2158
Burning velocity[d] ($cm.s^{-1}$)	237	42
Detonability range in air[c](%)	18 - 59	6.3 - 13.5
Energy of gaseous fuel explosion ($MJ.m^{-3}$)	9.9	32.3

a) NTP = normal temperature and pressure (293.15 K, 0.1013 Mpa).
b) 293.15 K, 0.1013 Mpa.
c) in a volumetric ratio.
d) a stochiometric mixture.

Table 2. Natural gas and hydrogen physical parameters at standard conditions (0 °C, 1 atm)

Property	Unit	Hydrogen	Natural gas
Lower caloric value	MJ/kg	121.03	48.02
Density	Kg/Nm^3	0.085	0.776
Molecular weight	g/mole	2.01	17.36
Wobbe number	MJ/Nm^3	45.88	62.03

Fuel Properties

Natural gas and hydrogen have different flammability, flame speed, and flame temperature depending on the gas quality regulation. A yearly average composition analysis of provided gas in Belgium (2020) is conducted to produce mean and standard deviation data for the individual gases. Physical parameters such as lower caloric value, density, molecular weight, Wobbe number, Net heating value, and Specific heat are calculated using the ISO 6976 standard and presented in table 2 and two percent inaccuracy in the caloric value is estimated by a minimum-maximum analysis (Fluxys – quality metrology). The Wobbe Index, heating value, and interchangeability are three of the most important characteristics of gaseous fuels. The heating value is strongly related to fuel kinetics and adiabatic flame temperature (T_{ad}). When natural gas is supplemented with hydrogen from 0 up to 30%, the heating value of the blends increases almost linearly and reaches 51.487 (MJ/kg). The most essential metric for measuring fuel gas interchangeability is the Wobbe Index, which is computed by dividing the volumetric value of the heating value under the stated reference conditions by the square root of the relative density at the same reference conditions. By increasing the hydrogen content by 30%, the Wobbe Index improves from 62.029 (MJ/kg) to 77.575 (MJ/kg) (25%) and will reach 458.726 (MJ/kg) if blending continues up to 100% hydrogen.

Combustion Parts

The IFRF is a turbulent diffusion burner that allows for external exhaust-gas recirculation and staged combustion, as well as changing the primary fuel supply position and swirl number. It can run at a lower excess air ratio with minimal emissions due to its recirculation (Chigier *et al*., 1972). The main roles of a burner are Turbulence, Time, and Temperature which relate to good mixing between fuels and air, ensuring complete combustion and assure ignition respectively (Jouret, 2021). In this section, the combustor (quartz) setup, swirl burner, and swirl generator are explained briefly. The diameter and length of the confinement are 255 and 310 mm, and the configuration works at atmospheric pressure. To quantify diverse flames, visual observation, and numerical inflame data are used. The IFRF designed and constructed an experimental natural gas swirl burner with multiple options for low NO_x investigations (Weber *et al*., 1992 and Driscoll *et al*., 1998). A cylindrical tube connects the swirl generator and burner quarl, and a moving block swirler provides an input swirl. The burner assembly is shown in figure 3. The burner quarl is built of refractory material and has a 20-degree opening angle.

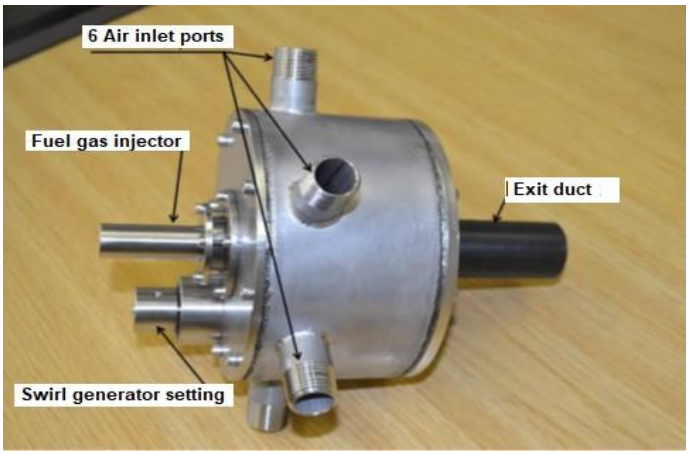

Fig 3. Burner assembly

A central fuel rod conducts the natural gas, which is injected radially in the swirling combustion air near the burner exit through a set of 24 holes (d_{hole} = 0.5 mm), creating an annular channel with D_0/D_{rod} = 27.18 mm. Natural gas is injected radially into the swirling combustion air through 24 holes ring set. There is a second annular slot between 1.20 D_0 and 1.33 D_0 that can be used to inject flue gas. The quarl is stepped 7.66 mm just above the fuel rod position and finally, 8 pipes with an internal diameter of 0.75 mm are provided to facilitate the injection of secondary fuel. The characteristic dimensions of the generic burner are shown in figure 4.

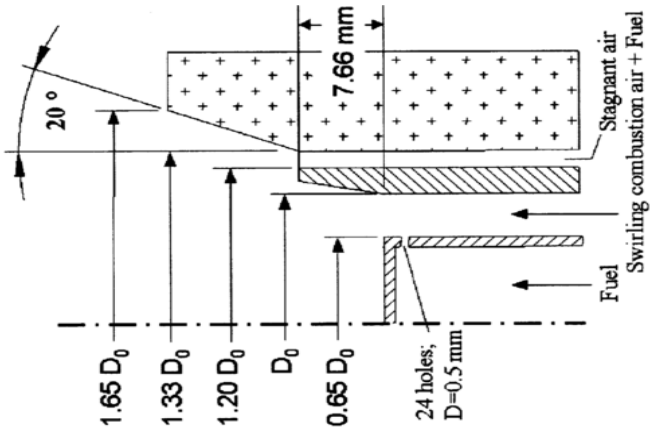

Fig 4. Characteristic dimensions of the generic burner for 30 kW, D_0 = 27 mm

Combustion

Combustion is an important process in human daily lives, such as driving a car, cooking on a gas stove, or lighting a candle, and to according to (El Hefni *et al*., 2019) combustion is a chemical reaction that occurs between a fuel and an oxidizing agent that produces energy, usually in the form of heat and light. Although combustion is beneficial in making our lives easier, it does have a drawback: pollution.

It is characterized by exothermic chemical reactions and can take place with or without a flame. Premixed, partially premixed, and non-premixed (diffusion) flame are the three types of flame modes. To offer flame stabilization, the burner has a cylindrical nozzle with a bluff body in the middle and can work with either premixed or non-premixed gases. In air combustion the fuel is natural gas, the oxygen is delivered by combustion air, and the heat is produced in a typical natural gas furnace. Studies have been conducted on methane/air combustion, including the GRI-Mech 3.0 mechanism (Frenklach *et al*., 1999) and those proposed by (Konnov and Hughes, 2001). Other researchers have also published data on methane-air combustion laminar burning velocity over a range of equivalence ratios at 1 atm. Using two blending spots at separate places, the mixing of natural gas and combustion air can be greatly varied, even if the stoichiometric ratio (SR) is maintained in most of the tests. The additional gas is injected radially into the swirling air and gas mixture at the second mixing spot or end of the fuel rod, resulting in a total power output of 30 kW in both cases. Fuels are often combusted with different amounts of air than the stoichiometric ratio. The equation of stoichiometry of oxygen/fuel reaction yields the theoretical air necessary for full combustion.

The minimum required air in a stoichiometric mixture is known as stoichiometric air, which can be used to compute the stoichiometric air/fuel ratio (AFR) (Vanoverberghe, 2004). Oxy-fuel combustion is the process of burning a fuel using pure oxygen, or a mixture of oxygen and recirculates flue gas, instead of air and it is now widely regarded as a cost-efficient and effective way to promote the technology in the industry (Ziębik and Liszka, 2010, Dumitras, 2004). However, the price of oxygen splitting from the air, CO_2 storage capabilities and transportation, and obtaining the so-called sequestered exhaust from the combustion are just a few of the major challenges associated with oxyfuel combustion (Plasynski *et al*., 2008, Golomb and Herzog, 2004, Stolaroff *et al*., 2006). Kimura *et al.* (1995) hypothesized that increasing gas temperature and oxygen content in flue gas can alleviate the combustion instability and increase the percentage of steam in the flue gas can improve the oxyfuel combustion efficiency (Kiga, 1995). The literature on instability in oxyfuel is limited. Ditaranto and Hals claimed that to achieve an adiabatic flame like that of fuel-air combustion temperature, oxygen volumetric concentration should be enhanced to a minimum of 30% (Hals and Ditaranto, 2006). They reported their findings on a laboratory-scale combustor, indicating that comparable instabilities happen in oxy-fuel combustion, potentially much more so than in traditional combustion.

However, once you pass this point, the instabilities become even more pronounced. It is possible to alter the oxidizer's composition in oxy-fuel combustion (the ratio between O_2 and CO_2). In comparison with conventional air combustion, this is the equivalent of adjusting the nitrogen-to-oxygen ratio, which is often difficult and costly.

Laminar Burning Velocities

Laminar flame speed is a key variable that describes the reactivity, diffusivity and exothermicity of a combustible mixture. This research looks at methane/air, hydrogen/ air, hydrogen-enriched in methane/air, oxy-dilution in methane/air, and hydrogen-enriched in methane/O_2/CO_2 mixtures. The burning velocity is a physicochemical property of a given flammable gaseous mixture (Andrews, 1972) and the LBV is the speed at which a flame front passes normally to its surface through unburned gas next to it. The flame's laminar burning velocity (S_L) can be expressed as:

$$S_L = (1/(A_c.\rho))\ (dm/dt) \qquad (2.1)$$

Where, *Ac* is the tube cross-sectional area of the, dm/dt is the unburned gas mass flow rate into the, and ρ is the unburned gas density next to the flame front (Rallis *et al*., 1980).

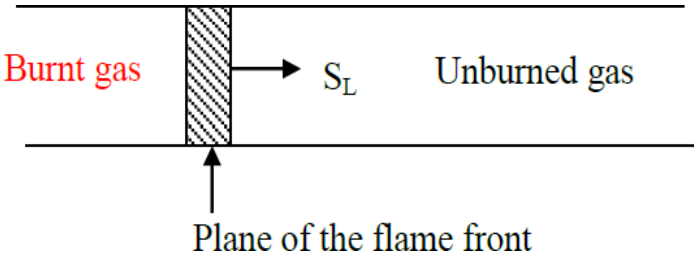

Fig 5. The plane front propagating diagram in an unconfined fuel mixture

Many experiments for evaluating the LBV of fuel and air blends have been designed and developed over the last decades, including the constant volume or pressure spherical flame method (Kelley *et al*., 2009, Lawes *et al*., 2000, Qin and Ju, 2005) counter flow or stagnation flame method (Wu and Law, 1985) heat flux method (Bosschaart *et al*., 2004, Coumans *et al*., 2013) heated diverging channel method externally (Akram, 2013) and annular stepwise tube method (Kim, 2011). Egolfopuolos *et al*. (2014) provided an important study of the stagnation/ counter flow burner technique, spherical flame propagation, and heat flux method. Combustion features including LBV of methane-air mixtures have been extensively reviewed and analyzed over several decades due to their simple molecular structure composition.

The influence of stretch on the LBV of a CH_4 and air mixture was originally examined in the seminal work of (Wu and Law, 1985). The greatest amplitude of LBV mixes is observed to exist for slightly rich mixtures and burning velocity declines along both sides of the stoichiometry. Disparities in the experimental results could be attributed to differences in observation and data extraction methodologies. Ogami and Kobayashi (2005), Ouitmette *et al*. (2009) and Mitu *et al*. (2017) all employed the Bunsen burner method to assess burning speed. The spherical flame method has been frequently utilized for measuring burning velocity. Because stretch is related to outwards propagating spherical flames, an adjustment is needed to acquire an exact burning velocity. Milton and Keck (1984) were the first to report experimentally obtained laminar burning velocity of hydrocarbon/hydrogen/air mixes as variables of T_u and P_u determined by using the constant volume spherical flame approach with no optical access and under stoichiometric situations. They found that the laminar burning velocity of the combination is smaller than the simple overall average of the laminar burning velocity of the individual components. Yu *et al.* (1986) broadened the methane-hydrogen-air mixture LBV research to off-stoichiometric mixes at ambient temperature and atmospheric pressure using the counter flow approach. They obtained a linear relationship between laminar burning velocity and hydrogen content.

Hermanns and Colleagues (2007) investigated the numerical and experimental examination of up to 40% hydrogen concentration in methane mixtures at ambient as well as higher temperatures and atmospheric pressure. They evaluated the impact of the burner plate as a potential catalyst using the heat flux (HF) technique and found no impact on the laminar burning velocity in the tested variable set. They also postulated a correlation for methane-hydrogen-air flames at increasing T_u, which was in good accord with the numerical simulation results. Plichta *et al.* (2013) investigated combinations of 50/50 and 10/90 percent of CH_4/H_2 in air, at 300 and 450 K and 1 atm, and 30/70 percent of CH_4/H_2 at 5 atm and 450 K, both burning in O_2:H_2 by 1:6. They validated the nonlinear influence of H_2 on LBV and contrasted experimental findings with Aramco Mech 1.0, finding excellent correlation in the lean and stoichiometric regions but an over-prediction in the fuel-rich area. Donohoe *et al.* (2014) evaluated the presented outcomes of (Plichta *et al.*, 2013) with Gri-Mech 3.0 and Aramco Mech 1.3, showing greater agreement than with the prior method. The LBV was calculated by a linear extrapolation approach in both papers. Cai *et al.* (2011) recently used a near-isotropic turbulence fan-stirred combustion chamber to investigate the influence of flame self-similar propagation and turbulent burning speed of methane-hydrogen-air mixes for a wide range of turbulence intensity. The normalized turbulent burning velocity rises dramatically as the efficient Lewis number of the mixture decreases. Furthermore, a strong self-similar propagation was seen because of the interaction between differential diffusion and flame stretch.

Heil *et al.* (2011) and Glarborg *et al.* (2012) studied the influence of CO_2/O_2 on the burning rates of methane oxyfuel combustion experimentally. It was discovered that the chemical effects of carbon dioxide existence have a considerable impact on the rates of CO_2 generation and consumption in oxyfuel combustion. Even though CO_2 effects on methane combustion have been extensively studied, the CO_2 dilution ratio in earlier research was low, and the highly diluted impact of CO_2 on CH_4 oxy-fuel mixtures is understudied. In addition, most studies have concentrated on the observation of flames, calculations of oxy-fuel flame speeds, and impact factor analyses and most of the experimental measurements are predicated on a constant oxygen concentration in the O_2/CO_2 combination. Typically, the findings are compared to the situation of fuel-air combustion. Current studies are still confined to oxy-fuel combinations with substantial amounts of CO_2 utilized as dilution. Furthermore, the research into the laminar burning speed and flame configuration of premixed combustible gas aims to gain a thorough understanding of the combustion properties and chemical reaction kinetics characteristics of various types of fuels, which will aid in the optimization of the combustion and increase its effectiveness, and lowering emissions. Another useful parameter for describing various combustion processes is the laminar flame velocity (flame stability, blowing, flashback, and extinguishing). As a result, integrating experiments and numerical modeling to investigate flame speed and structure can provide insight into the combustion process, an understanding of the turbulent combustion process, and vital data for creating surrogate fuel models and verifying turbulence models.

Methodology

The proposed experimental setup in this work consists of six main components (see appendix 1 and 2). Combustion chamber (1) has quartz walls and a swirl burner is placed in it. Air and natural gas supplied from the grid (2) are used in phase I to ensure that the future experimental setup is working properly. The third part ensures fuel (CH_4, H_2) and oxidizer (O_2, CO_2) are available from gas bottles (3). The control system is built utilizing operational data collected by sensors (4) to ensure the safe operation. The extraction system (5) is the fifth part, which dilutes and ejects the hot exhaust gases outside the lab.

Finally, the measurement devices, which are used to diagnose the flame (6), complete the set-up. The gas supply chain is separated into two phases. Phase I consists of natural gas and air, which are both supplied by a local grid. Phase II covers the entire scope, using methane and hydrogen as fuels and air, oxygen, and carbon dioxide as oxidizers, with all gases coming from gas bottles.

Natural Gas and Compressed Air Supply System - Phase I

The major goal of phase I is to optimize the installation and gain experience before proceeding to Phase II. Phase I also provides for the validation of the primary equipment. Natural gas is supplied by the low-pressure grid on the fuel side (25 mbar) and the supply chain was designed with risk analysis and safety standards for gas burners in mind. The supply line is constructed on a panel that is connected to the frame under the combustor. Manual valves, manual shut-off valves, manual control valves, flow sensors, and check valves are all included in the system.

Fuel and Oxidizer Supply System - Phase II

After completing phase I, the supply chain will be modified to allow the installation to be fed by gas bottles. Phase II involves supplying and mixing methane and hydrogen in the fuel direction as well as air, oxygen, and carbon dioxide in the oxidizer direction within the gas mixing station. The major goal in phase II is to adjust the fuel mixture composition as well as some operational factors including swirl, equivalence ratio, fuel staging ratio, combustion air temperature, and thermal load. The pressure reduction system is attached to the gas bottles and lowers the gas pressure to 6 to 10 bar and the system is made up of safety valves, manual valves, and shut-off valves. On the oxidizer side, the blend consisting of air, oxygen, and carbon dioxide is first mixed before flowing through the air preheater. The whole installation is mounted on a fixed panel, in a well-ventilated area. It consists of flow strainers, mass flow controllers, check valves, shut-off valves, manual valves, flame arresters, and pressure and temperature sensors. The exhaust gases leave the combustion chamber at a high temperature, around 1300 ˚C, as determined by (Koen Vanoverberghe, 2004) in previous experiments. The flue gases are removed using an extraction system, which ensures that the flue gases cool down due to a considerable dilution with the surrounding air and covers the extraction's temperature and flue gas emissions. At maximum load (30 kW), the extreme situation for the flue gas at the combustor output corresponds to stoichiometric combustion (no extra air) in adiabatic conditions (no heat losses).

In air-combustion mode, the equivalent flow rate and temperature are 33 Nm^3/h (normal cubic meter: Temperature: 0 ˚C, Pressure: 1.01325 bar A) and 2155˚C, respectively, whereas, in oxy-combustion mode, it is just 24 Nm^3/h and 2100 ˚C. To achieve a temperature of 90 ˚C after dilution, the required airflow is about 1100 Nm^3/h with an ambient temperature of 20 ˚C. The minimum airflow becomes 3000 Nm^3/h if the temperature after dilution is 45 ˚C.

Laminar Burning Velocity

Experimental methods for evaluating laminar burning velocity have been established for many decades. Stationary flames and propagating flames are the two types of experimental procedures. LBV is measured using stationary flames by injecting a premixed flammable gaseous mixture into a stationary flame front as laminar flow and the velocity of gaseous flow equals the velocity of laminar burning (Rallis *et al*., 1980 and Dahoe *et al*., 2003). However, since the stationary flame front is unstable, ensuring that a flame front is an ideal plane is difficult. CHEMKIN software can be used to simulate flame velocity numerically. The following section contains a review of previous measurements and investigations on laminar burning velocity as a survey to have a better idea about the next steps of this paper.

Methane-Air Mixtures

Ulinski *et al*. (1998) conducted an experimental examination of the LBV of methane-air mixtures with a constant volume combustion vessel, and the results demonstrated it for methane-air gaseous mixtures at various pressures (1.0 - 3.0 atm) and temperatures (298 - 500 K).

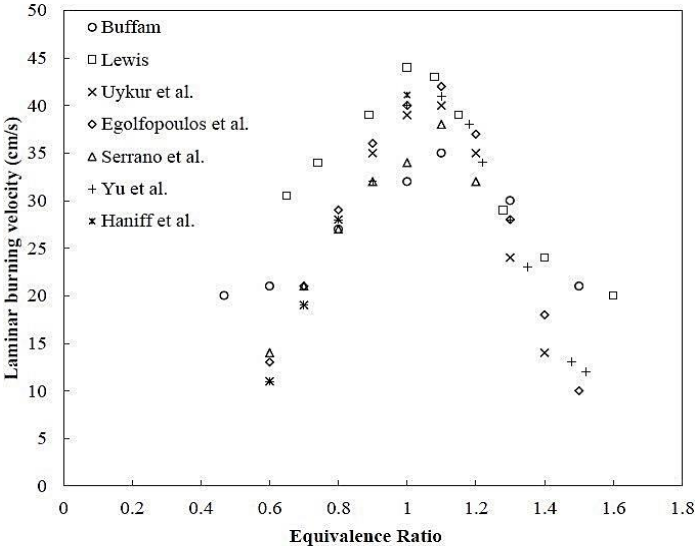

Fig 6. LBV comparison of the CH_4-air mixture

Their research focused on the LBV of methane-air diluent mixtures for ϕ between 0.65 and 1.1 and 0 - 10 % diluents. Ulinski's research found that the maximum LBV of a methane/air mixture is 0.35 m/s at ϕ = 1.03, whereas Egolfopoulos et al. discovered that the maximum LBV of a methane-air mixture is in the range of 37 to 43 cm/s at ϕ = 1 (Egolfopoulos, 1989). Figure 3.1 provides an LBV comparison of CH_4/air from several investigations. Lewis' bell-shaped association between burning velocity and equivalence ratio suggests that the maximum laminar burning velocity for a methane-air mixture is 44 cm/s at an equivalence ratio of one (Lamoureux, 2003). It has been discovered that methane-air mixture velocity is in the range of 32 - 44 cm/s at an equivalence ratio of near one.

Hydrogen-Air Mixture

Prior research has measured and numerically modeled the hydrogen/air LBV, with the greatest combination varied between 250 and 350 cm/s (Milton, 1984, Liu, 1983, Crayford, 2006, Forman, 2009 and Duan, 2020). Figure 7 shows a comparison of these investigations at atmospheric pressure and 293 K and over a range of equivalence ratios, with the highest amounts ranging from 290 cm/s to 350 cm/s.

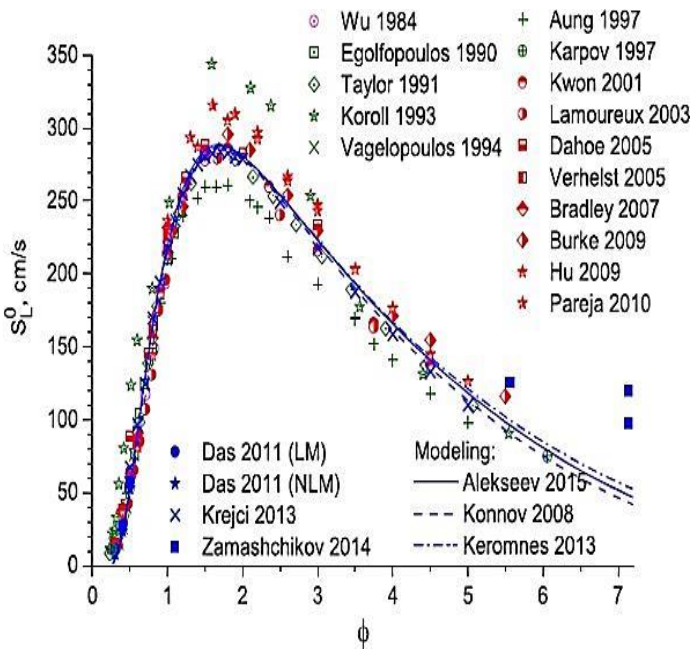

Fig 7. The comparison of H_2 -air mixture laminar burning velocity

Hydrogen Enriched in the Methane-Air Mixture

Laminar burning velocity measurements for H_2-CH_4 mixtures were undertaken by (Ilbas *et al*., 2006) at ambient temperatures. With the addition of hydrogen, the laminar burning velocity of H_2-CH_4 starts to rise.

The magnitude of the increase is mostly determined by the hydrogen content. Figure 8 shows that the effect of increasing burning velocity in hydrogen methane mixtures reduces slightly within 20% of hydrogen content, but with an increase of hydrogen concentration over 70%, the burning velocity rises significantly (Dahoe, 2003).

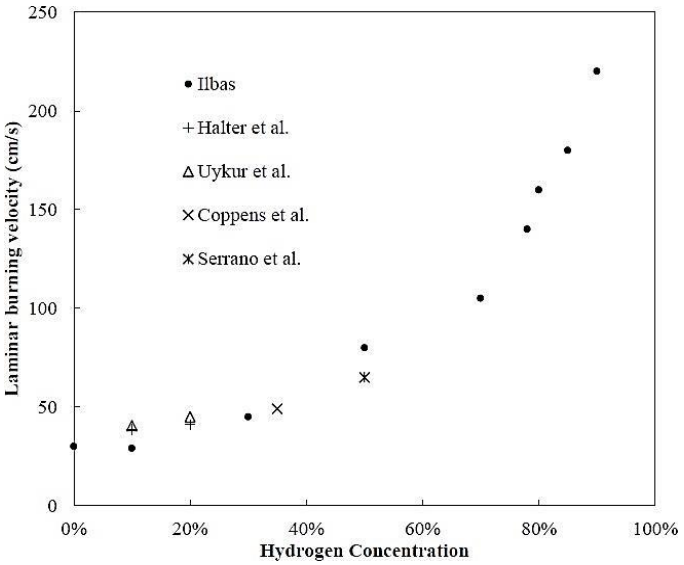

Fig 8. The impact of hydrogen proportion on the LBV of the H_2 -CH_4 at the stoichiometric condition

Oxy-Dilution in the Methane-Air Mixture

As shown in figure 9, the laminar flame speed of methane-air fell dramatically as the proportion of CO_2 increased, and the changing trend was nonlinear. This was mostly due to the FCO_2 dilution and heat effects. To estimate their relative impact (Halter *et al*., 2009) performed simulations by introducing a new molecule (F-CO_2, for 'False' CO_2) that possesses the thermal and transport characteristics of carbon dioxide but is chemically inactive. The heat and mass transfer rate between both the burned and unburned gas reduced throughout combustion due to the lower Soret diffusion effect. Additionally, increasing the CO_2 concentration reduces the reactant content of the methane/air, which reduces the effective collision probability of the methane and oxygen molecules, causing a drop in the methane/air flame speed.

Methane- CO_2/ O_2 Mixture

Observations of laminar flame speeds of CH_4/O_2/CO_2 blends were plotted as a function of equivalence ratio (from 0.6 to 1.4) with various O_2 concentrations in figure 3.5. (from 25 % to 35 %). The maximum flame speeds were 11.1, 15.7, 20.0, 26.1 and 29.6 cm/s, corresponding to O_2 concentrations of 25, 29, 31, 33, and 35%.

Data fitting revealed a quadratic function relationship between flame speeds and O_2 concentrations, with all squared correlation coefficients (R^2) above 0.98.

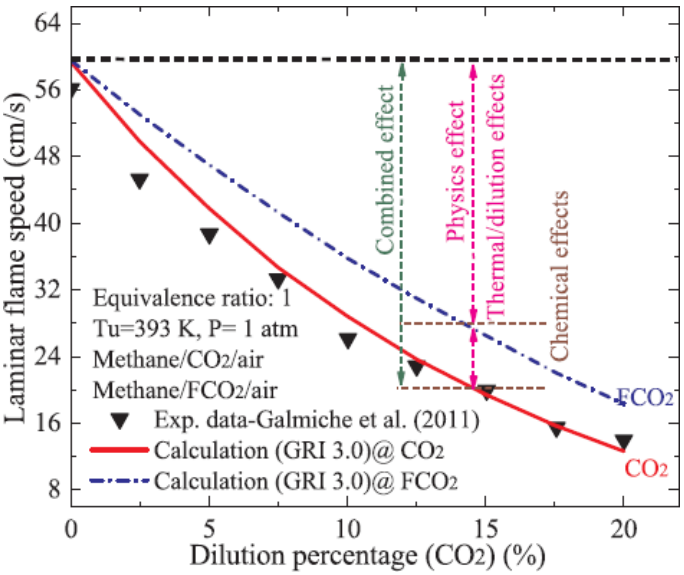

Fig 9. The effects of CO_2 (dilution) on the methane-air laminar flame speed

The adiabatic flame temperature of the $CH_4/CO_2/O_2$ mixture at various equivalence ratios is depicted in figure 11. This temperature has a large effect on elementary reactions, and varied adiabatic flame temperature corresponds to different reaction rate constants (Zhang, 2013). Previous research has shown that the thermal impact of CO_2 can be examined by adiabatic flame temperature (Kim, 1996). For all equivalence ratios, the adiabatic flame temperature decreases with the addition of CO_2, although it does not fall linearly with the rise of the CO_2 fraction. However, the mixture exhibits a stronger thermal effect under lean or rich conditions than under stoichiometric ones.

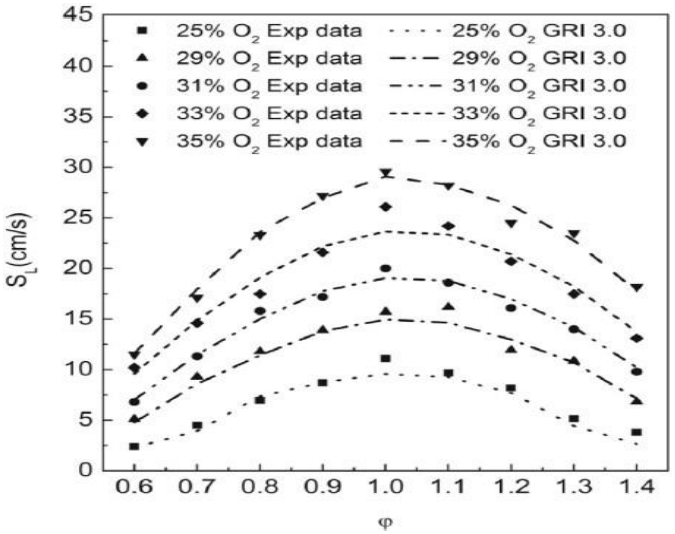

Fig 10. The speed of a laminar flame as a function of equivalence ratio

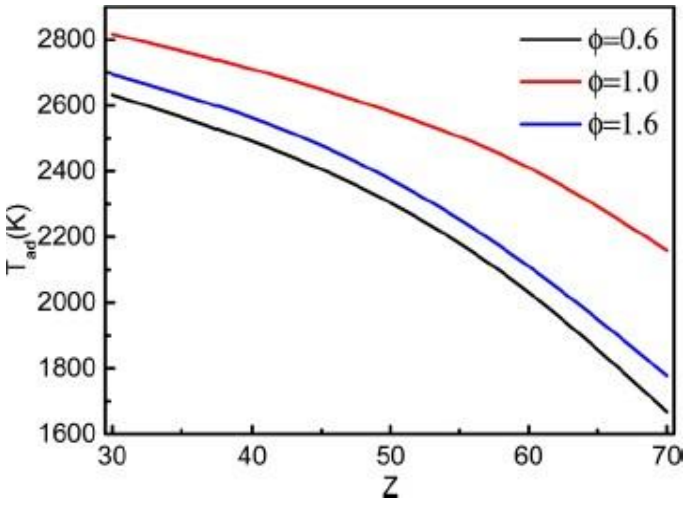

Fig 11. Adiabatic flame temperature of the mixture for different equivalence ratios (Z) at P = 0.1 MPa

Results and Discussion

PFD and P&ID

The Process Flow Diagram (PFD) and Piping/Process and Instrumentation Drawing (P&ID) are used in this project to define or explain the complex flows, tube sizes, equipment, fuel and air supply, and instrumentation that exist in a designed unit. The process flow diagram's objective is to define the process's design and it is a basic illustration of a process that displays the conversion of raw materials to end products schematically. This diagram shows the flow of chemical fluids and the equipment involved in the process with the properties of flowing chemical fluids. In other words, a process flow diagram is a detailed schematic representation of the general flow, important equipment, and materials involved in each industrial operation, as well as the working fluid (see appendix 3). In this project, P&ID includes all major equipment, tubing details, flow rate and instrumentation details like pressure, temperature, different valves, mass flow controllers, mass flow meters, and combustor. The major and minor flows, control loops, and instrumentation are all included in P&ID and the proposed P&ID for this project will be used for all series of tests. The general scope of the project and the scope of the external supplier are represented in appendix 4 and 5, respectively. More information about the flow rate calculation, tube sizing calculation and external suppliers are provided in the following section.

Flow Rate

The set-up included fuel and oxidizer lines to feed gaseous fuels, air, and/or O_2 + CO_2 mixtures to the burner. Bottled gases of methane and hydrogen were used to prepare the desired fuel mixture.

Compressed air, bottled oxygen and carbon dioxide were used to prepare the oxidizer mixtures necessary to achieve conventional or distributed combustion conditions. When more air is injected into the system than is required (lean combustion), the combustion efficiency improves modestly at first, but thereafter declines completely. When excess air levels increase combustion effectiveness at first rises and then falls, which is thought to be related to an increase in CO_2 and hydrocarbon emissions. The test facility is designed to burn a fuel mix made of natural gas and hydrogen, with 3 types of oxidizer flows, namely air, oxygen-enriched air, and O_2 diluted with CO_2. The supply of the gases comes either from a grid (Natural gas at 25 mbar and compressed air at 7 bar) or gas bottles (CH_4, H_2, O_2 and CO_2 at 175, 200, 200 and 50 bar, respectively).

Table 3. Flow rate calculation of natural gas

Parameter	Unit	Value
Load	kW	30
Natural gas LHV	kWh/Nm^3	10.36
Gas flow	Nm^3/h	2.9

Table 3 describes the calculation of the maximum natural gas flow rate. Dividing the maximum thermal load by the natural gas lower heating value (LHV) yields the maximum natural gas flow rate.

Table 4. Flow rate calculation of stoichiometric combustion

Gas	Volumetric Flow Rate (Nm^3)	Mass Flow Rate (kg/h)
Natural gas flow	2.9	2.2
Air flow	28.2	34.6
O_2 flow	5.9	8.0
CO_2 flow	13.8	25.9
Hydrogen flow	10	0.9
Air flow	23.8	29.2
O_2 flow	5.0	6.8
CO_2 flow	11.7	21.8
Methane flow	3.2	2.2
Air flow	30.2	37
O_2 flow	6.3	8.6
CO_2 flow	14.8	27.7

Table 4 shows the gas volumetric and mass flow rates at the maximum thermal load (30 kW) in the system. The ratio of real airflow to stoichiometric airflow is called lambda (λ). Lambda is often slightly positive in conventional burners, equaling 1.15. According to the complete combustion of stoichiometric equation (Eq 4.1), 3.2 Nm^3methane, 2.9 Nm^3 natural gas and 10 Nm^3 hydrogen are required as the fuel and finally volumetric and mass flow rates are calculated based on stoichiometric equations. System safety depends on maintaining appropriate air-fuel mixture control. If the mixture is too lean, and the temperature falls below the required ignition temperature, the flame will blow out. It is also critical to keep the air mass flow rate in proportion to the gas mass flow rate (no lack of air):

$$(\boldsymbol{CH_4 + 2(O_2 + 3.76\, N_2) - - > CO_2 + 2\, H_2O + 7.52\, N_2}) \qquad (4.1)$$

The matrix of completed experiments is illustrated in appendix 6. It contains the outcome of the hydrogen addition to natural gas in a 30 kW burner for the same input heat. Following the calculation of the ratio in the system, six steps are defined to evaluate various stages, as indicated in table 5. The table depicts the different steps to supply gas and air lines together. In other words, it specifies the proportion of each gas in each situation and allows for comparisons. Three different % of methane and hydrogen are defined (0, 50 and 100 %). Method A uses natural gas and air combustion, whereas methods B and C use hydrogen-enriched natural gas, with method C reaching 100% hydrogen. Oxy-combustion is also demonstrated in methods D to I. Natural gas testing with various concentrations of O_2/ CO_2, as well as hydrogen-enriched natural gas, are included in methods D and G, as well as hydrogen-enriched natural gas in methods E, F, H, and I. In appendix 7, it shows that with a 30 kW input, the burner requires 2.9 Nm^3/h natural gas or 3.2 Nm^3/h methane. The maximum calculated volumetric flow rate of methane and hydrogen is shown in the first portion of the table. The needed oxidizer flow rate is then shown using previously determined equivalence ratios (0.4 – 1.2). Increases in the equivalence ratio and hydrogen % reduce oxidizer flow rates, as seen in the table below. Based on this calculation, we can extract maximum and minimum flow rates at 30 kW in the following tables.

Table 5. Defined scenarios to test the mixing system

Scenario		A	B	C	D	E	F	G	H	I
Methane	%	100	50	0	100	50	0	100	50	0
Hydrogen	%	0	50	100	0	50	100	0	50	100
Air	%	100	100	100	0	0	0	0	0	0
O_2/CO_2	%	0	0	0	100	100	100	100	100	100
O_2	%	0	0	0	30	30	30	15	15	15
CO_2	%	0	0	0	70	70	70	85	85	85

Table 6. Flow Rate (Nm^3/h) - MAX value at 30 kW

Phi	1.2	1	0.8	0.6	0.4
CH_4	3.2	3.2	3.2	3.2	3.2
Hydrogen	2.4	2.4	2.4	2.4	2.4
H_2+CH_4	4.8	4.8	4.8	4.8	4.8
Air	25.6	30.2	37.8	50.4	75.6
Oxygen	5.4	6.3	7.9	10.6	15.9
CO_2 (30%O_2)	12.6	14.8	18.5	24.7	37
CO_2 (15%O_2)	30.5	36	45	60	89.9

Table 7. Flow Rate (Nm^3/h) - MIN value at 30 kW

Phi	1.2	1	0.8	0.6	0.4
CH_4	2.4	2.4	2.4	2.4	2.4
Hydrogen	0	0	0	0	0
H_2 + CH_4	3.2	3.2	3.2	3.2	3.2
Air	24.3	28.7	35.9	47.8	71.7
Oxygen	5.1	6	7.5	10	15.1
CO_2 (30%O_2)	11.9	14.1	17.6	23.4	35.1
CO_2 (15%O_2)	28.9	34.1	42.7	56.9	85.3

Tube Sizing

The optimum tube size for the system has been chosen based on the proposed P&ID. According to the literature, there are several ways, formulas, and calculators for defining and optimizing tube size in each line, therefore we compared and chose the best available size for the system by using multiple approaches at the same time. Since the pressure at the mass flow controller outlet is reduced, it's important to calculate tube size at both the input and output of the mass flow controllers, which usually results in a larger size at the outlet. As a result, we may need to build different tube sizes before and after the mass flow controller in some circumstances. Steel tubes provided for this system are based on Sandvik 3R60T M, standard ASTM: TP316L, TP316. The calculation results of different methods are mentioned in the following table. According to results in table 8 as well as the consultant with different suppliers, the variety in size selection is almost high (five different sizes from 6 to 22 mm) which increases construction cost, lead time as well as difficulty in system connection.

Table 8. Tube size at the inlet and outlet of MFC

Component	Pipe Size via Fluid Velocity [81]	Poiseuille or Hagen-Poiseuille Law	Limiting Velocity [82]	Simulator Calculation	Specific Volume	Optimum Size	
Tube Size at the Inlet of MFC							
Air	3/4"	1/4"	1/4"	3/4"	1/2"	1/2"	12 mm
O_2	3/8"	3/16"	1/8"	3/8"	5/16"	3/8"	9 mm
CO_2	7/8"	1/4"	1/4"	7/8"	5/8"	1/2"	12 mm
CH_4	1/4"	1/8"	1/16"	1/4"	3/16"	1/4"	6 mm
H_2	1/4"	1/8"	1/16"	1/4"	3/16"	1/4"	6 mm
O_2 + CO_2	2"	1/2"	3/4"	2"	7/8"	7/8"	22 mm
CH_4 + H_2	5/8"	1/4"	3/16"	5/8"	1/4"	3/8"	9 mm
NG grid	1/2"	1/4"	3/16"	-	1/4"	3/8"	9 mm
Tube Size at the Outlet of MFC							
Air	1 3/4"	1/2"	5/8"	1 3/4"	3/4"	7/8"	22 mm
O_2	7/8"	3/8"	5/16"	7/8"	1/2"	3/4"	18 mm
CO_2	1 3/4"	1/2"	3/4"	2"	7/8"	7/8"	22 mm
CH_4	1/2"	1/4"	3/16"	1/2"	1/4"	3/8"	9 mm
H_2	1/2"	1/4"	1/8"	1/2"	3/16"	3/8"	9 mm
CH_4 + H_2	5/8"	1/4"	1/4"	5/8"	1/4"	3/8"	9 mm
NG grid	1/2"	1/4"	3/16"	-	1/4"	3/8"	9 mm

Therefore, another optimization is performed in tube sizing. At this stage, we perform a new calculation based on economic flow velocities in pipelines for various media in m/s (guide values) related to the condition in the pipeline which is provided in Appendix 8. In this method, we use volumetric flow rates and pipe size via fluid velocity equation (Menon, 2005) to calculate economic flow velocity at different equivalence ratios (0.4 – 1.2). According to different applications in this method, we choose three sizes (4, 12 and 25 mm tube ID) for the system's inlet and outlet of mass flow controllers, which are covered within defined ranges in most situations (table 9). Since the pressure inside the natural gas line is very low (25 mbar), we must select a bigger steel pipe in this line based on economic flow velocity and maximum pressure loss. Galvanized steel pipes (also known as galvanized steel sleeves) fulfill the above requirements and are hot dip galvanized at the manufacturer to NBN EN 10240 standards.

Table 9. Tube sizing based on economic flow velocities in pipelines for various media in m/s

Component		Tube Size	Guidelines		Gas Speed in Tube				
		ID	Min	Max	1.2	1	0.8	0.6	0.4
		mm	m/s						
Inlet	Air	25	2	10	2.2	2.6	3.3	4.4	6.5
	O_2	12	2	10	2.0	2.4	3.0	4.0	6.0
	CO_2 (30%O_2)	12	2	10	4.7	5.6	6.9	9.3	13.9
	CO_2 (15%O_2)	12	2	10	11.4	13.5	16.9	22.5	33.7
Outlet	Cold Air	25	10	40	14.1	16.6	20.8	27.7	41.5
	Hot Air		10	40	23.1	27.3	34.1	45.5	68.2
	O_2	25	10	40	3.0	3.5	4.4	5.8	8.7
	CO_2 (30%O_2)	25	10	40	6.9	8.1	10.2	13.6	20.4
	O_2+CO_2 (30%O_2)	25	10	40	9.9	11.6	14.5	19.4	29.1
	Hot O_2-CO_2	25	10	40	16.2	19.1	23.9	31.8	47.8
	CO_2 (15%O_2)	25	10	40	16.8	19.8	24.7	33.0	49.4
	O_2+CO_2 (15 % O_2)	25	10	40	19.7	23.3	29.1	38.8	58.2
	Hot O_2-CO_2		10	40	32.4	38.2	47.8	63.7	95.5
Inlet	CH_4	4	5	15	10.7	10.7	10.7	10.7	10.7
	H_2	4	5	15	8.1	8.1	8.1	8.1	8.1
Outlet	CH_4	12	3	10	7.6	7.6	7.6	7.6	7.6
	H_2	12	3	10	5.7	5.7	5.7	5.7	5.7
Inlet	CH_4+H_2	12	3	10	11.5	11.5	11.5	11.5	11.5
Outlet	CH_4+H_2	25	0.5	1	2.8	2.8	2.8	2.8	2.8

Table 10. Natural gas tube sizing based on economic flow velocities in pipelines (m/s)

Guidelines		Gas Speed in Tube				
Min	Max	1.2	1	0.8	0.6	0.4
0.5	1	4.8	2.5	1.6	0.9	0.7
Code		DN15	DN20	DN25	DN32	DN40
Size		1/2"	3/4"	1"	1 1/4"	1 1/2"
OD	mm	21.3	26.9	33.7	42.4	48.3
Wall thickness	mm	3.2	3.2	4	4	4
ID	mm	14.9	20.5	25.7	34.4	40.3
Density	kg/Nm^3	0.7767				
Viscosity	Pa.s	0.0001				
Reynolds	-	543.0	394.7	314.8	235.2	200.8
Length pipe	m	10				
Pressure Loss Coeff (pipe)	-	79.1	79.1	79.1	79.1	79.1
Pressure Loss Coeff (Valve & bend)	-	79.1	79.1	79.1	79.1	79.1
Pressure Loss	Pa	1421.1	396.6	160.6	50.0	26.6
Pressure Loss	mbar	14.2	4.0	1.6	0.5	0.3

The NBN standard is used to determine the best tube size for natural gas lines, which is 1 inch or 25 mm ID (table 10). Based on previous calculations, only three different sizes are selected according to the new sizing approach, which is a more optimal strategy than the previous one and reduces construction costs. The final tube sizing design will be shown below:

Suppliers and Equipment

Different suppliers provide design, engineering, consulting, delivery, training, and after-sales services to implement desired P&ID. In addition, when contacting suppliers, some crucial parameters for the customer or research group must be considered. Lead time, cost, design coherence, and similarity to the target system are all important considerations. Eight different companies have submitted their quote for the proposed P&ID in this project. Four companies provided installation skids and fitting systems, while the rest exclusively provided mass flow controllers and mass flow meters. A comparison between different companies is performed in table 11. It is worth noting that the P&ID has been modified several times and cooperation with some suppliers was finished after the first quotation.

The system was ordered by a combination of D and H companies after considering the effective parameters, existing difficulties and the supplier's terms.

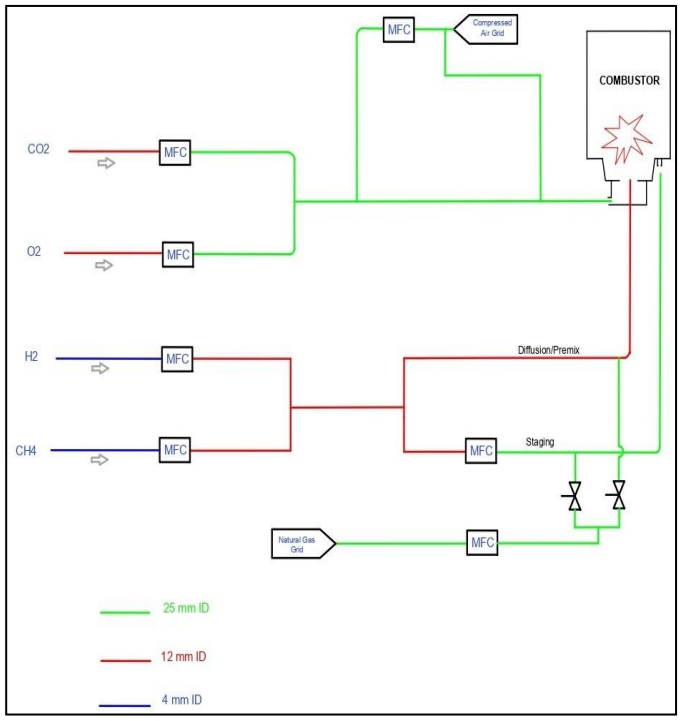

Fig 11. Final tube sizes to design the system

Table 11. Flow rate calculation of stoichiometric combustion

Supplier	Price (€*1000)	Lead Time (Weeks)	Equipment
A	16.2	11	7 MFC - fitting – power adapter - software
B	12.2	8	6 MFC
C	20.7	16	5 MFC – 2 MCV- adapter - power supply
D	16.9	20	5 MFC - 2 MCV
E	52.3	25	Skid
F	17830	25	Skid equipment - fitting
G	36500	20	Skid
H	26400	20	Skid

Conclusion and Recommendation

This study includes the design of a gas supply and mixing station for the combustor test facility, as well as the laminar flame speed investigation.

The scope and aims of this study have been determined in the introduction, which is an optimal and cost-effective gaseous fuel mixing system for research activities and a combustor test facility that will be able to burn natural gas with the addition of hydrogen, air and oxy-combustion based on the oxygen fraction. Furthermore, to understand the specification and composition of gases, as well as the combustion part, a literature review has been conducted. Even though this technology has been there for a few decades, it was discovered that the concept of hydrogen-enriched oxy-combustion is relatively new in terms of the few experimental research that has been done in this field. The proposed P&ID for this project, which includes two phases, is based on the calculation of flow rate, tube sizing, and available quotations from suppliers to have a more effective system with optimal construction costs. The final version of the P&ID phases contains the panel for the gas mixing and the panel for the gas split system. The optimization and balancing of the flow rate and tube sizing was a practical challenge for the author. After the completion of the system design, eight different suppliers were evaluated in the ordering process.

They are classified into two groups: companies that provide Mass Flow Controllers/Meters as the principal equipment in our system and companies that provide assembly on a panel to place and fit equipment together. In the next step, the study investigated the methane-air, hydrogen-air, hydrogen-enriched in methane-air, oxy-dilution in the methane-air mixture and methane CO_2/ O_2 mixture to see how they affect laminar flame speed.

The following conclusions were summarized in this section:

- The impact of carbon dioxide dilution gas had the biggest impact on the adiabatic combustion temperature, laminar flame speed, and crucial radicals' generation of the methane-air. At an equivalence ratio of about one, the LBV in methane-air mixtures is in the region of 32-44 cm/s.
- The laminar burning velocity of hydrogen-air combustion at atmospheric pressure and 293 K includes a wide range of equivalence ratios, ranging from 210-280 cm/s at an equivalence ratio of 1. The greatest values with an equivalence ratio of 1.6 range from 290 cm/s to around 350 cm/s.
- The addition of hydrogen increases the methane-hydrogen-air mixture's laminar flame speed and adiabatic combustion temperature. Additionally, the lean-burn limitation was expanded by increasing the hydrogen ratio in the methane/air combination.
- The laminar burning velocities of CH_4-CO_2-O_2 attained a maximum at an equivalence ratio of one and then decreased on either side.

- Furthermore, as the CO_2 content in the oxidizer increases, the laminar burning velocities of $CH_4/CO_2/O_2$ decrease. The highest laminar flame speeds improved as the O_2 concentration increased, with 11.1 and 29.6 cm/s corresponding to O_2 concentrations of 25 and 35% respectively.
- To conclude it can be stated that the addition of hydrogen can increase the laminar flame speed. As a result, optimizing the percentage of oxygen and hydrogen in the mixture and performing simulations in future works is recommended.

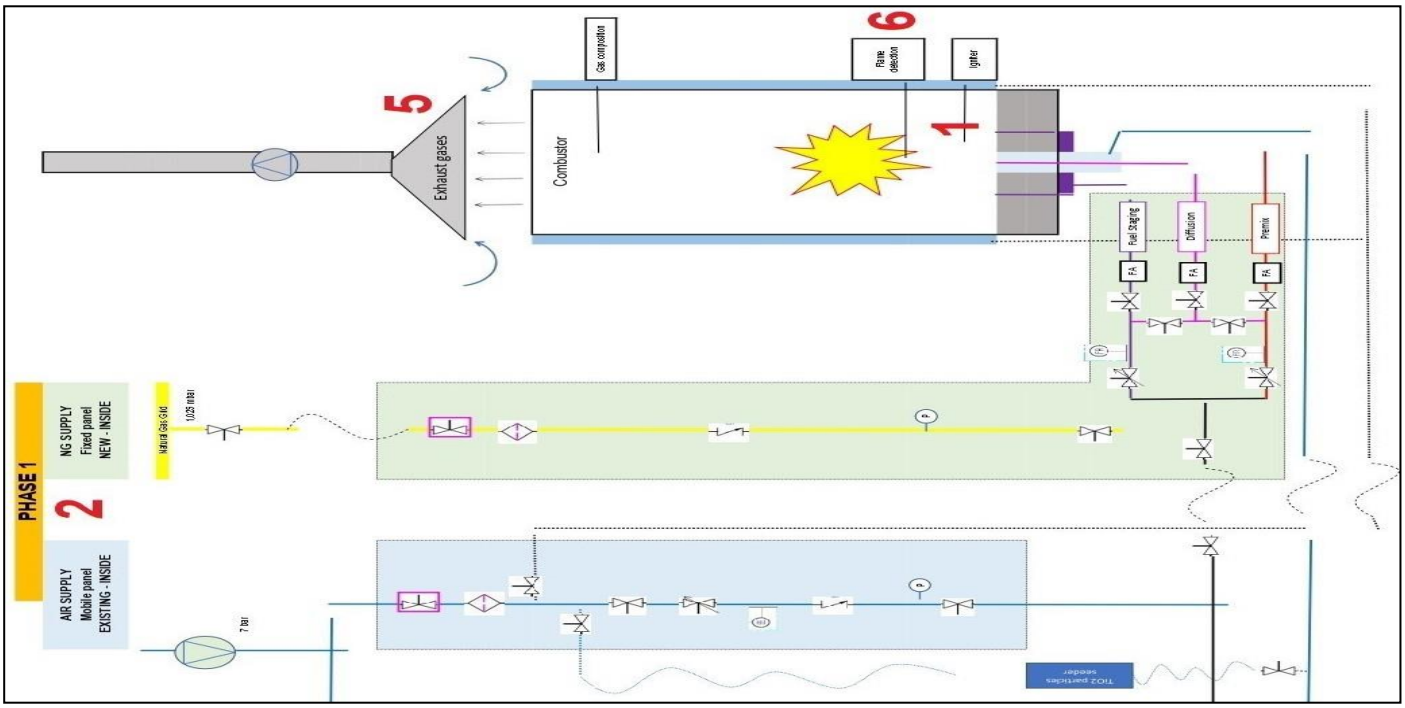

Appendix 1. Test facility Layout – Phase 1

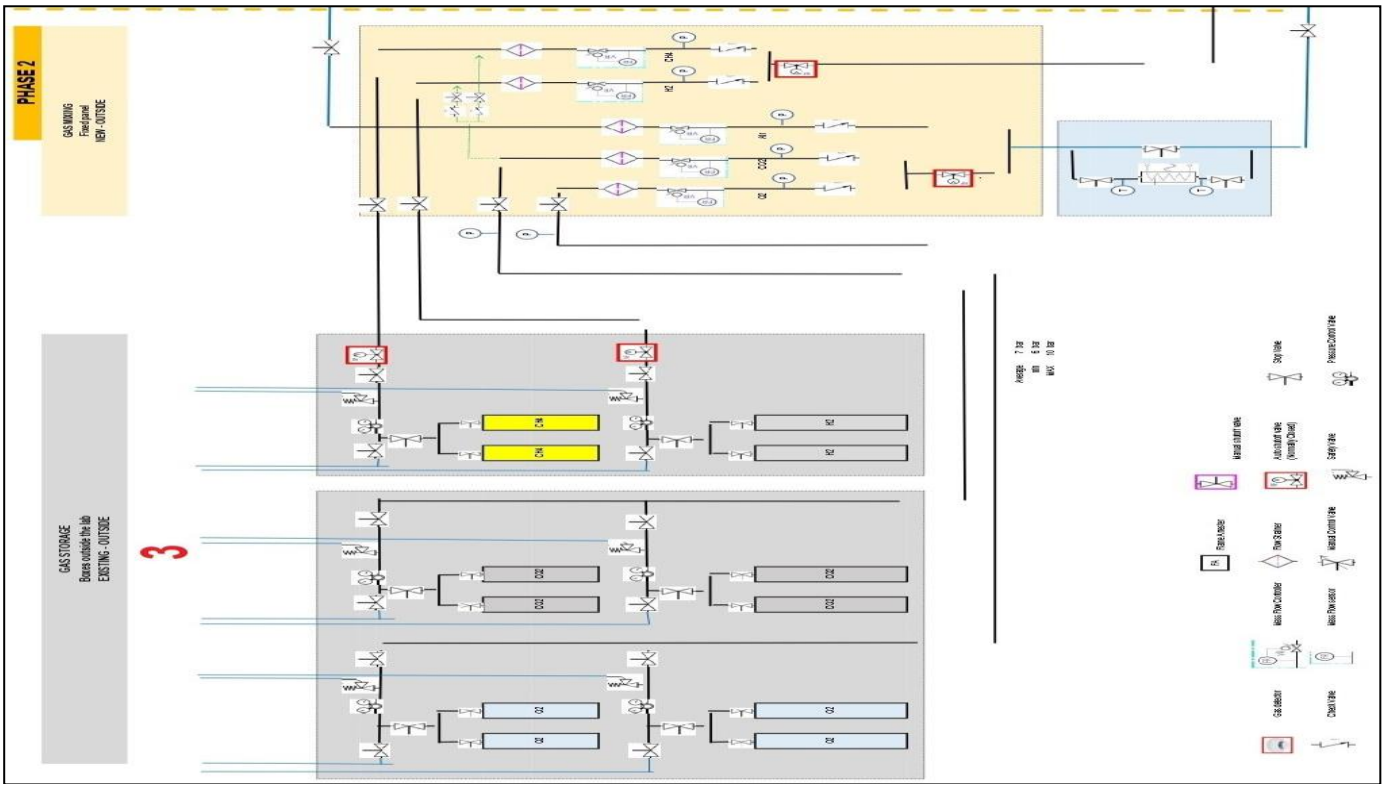

Appendix 2. Test facility Layout – Phase 2 and gas storage

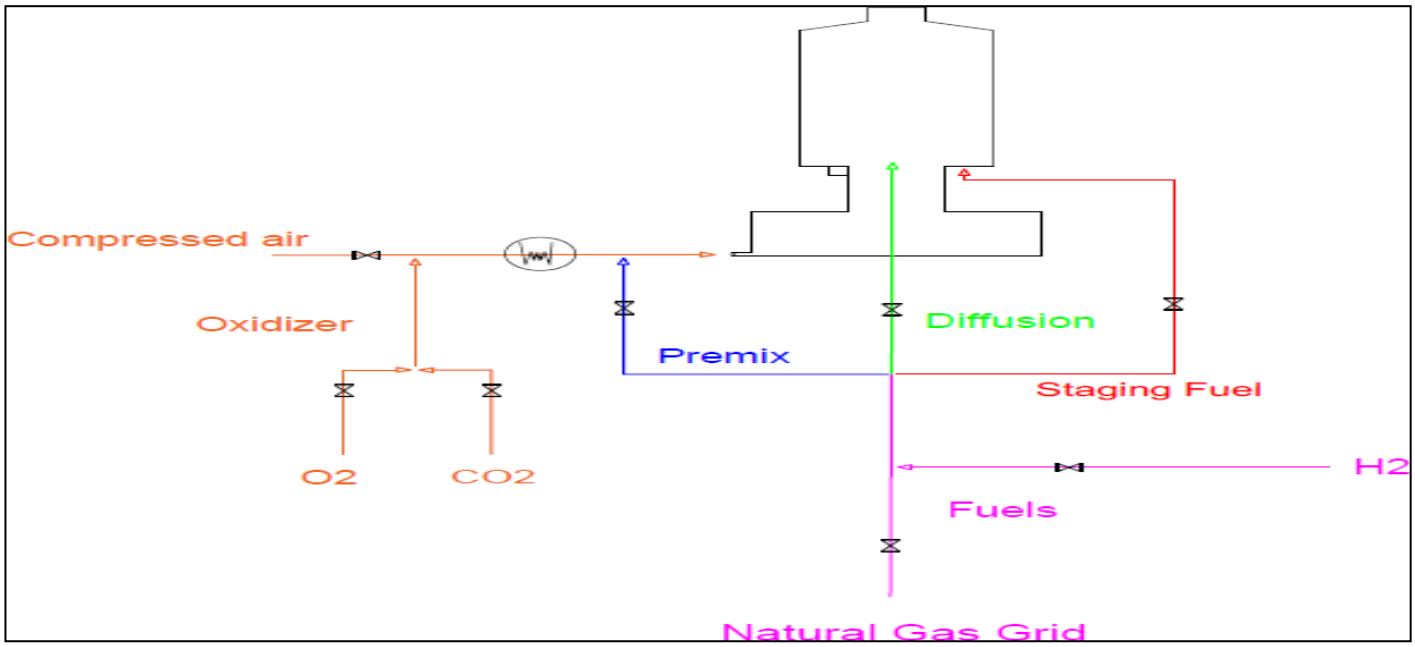

Appendix 3. Process flow diagram (PFD)

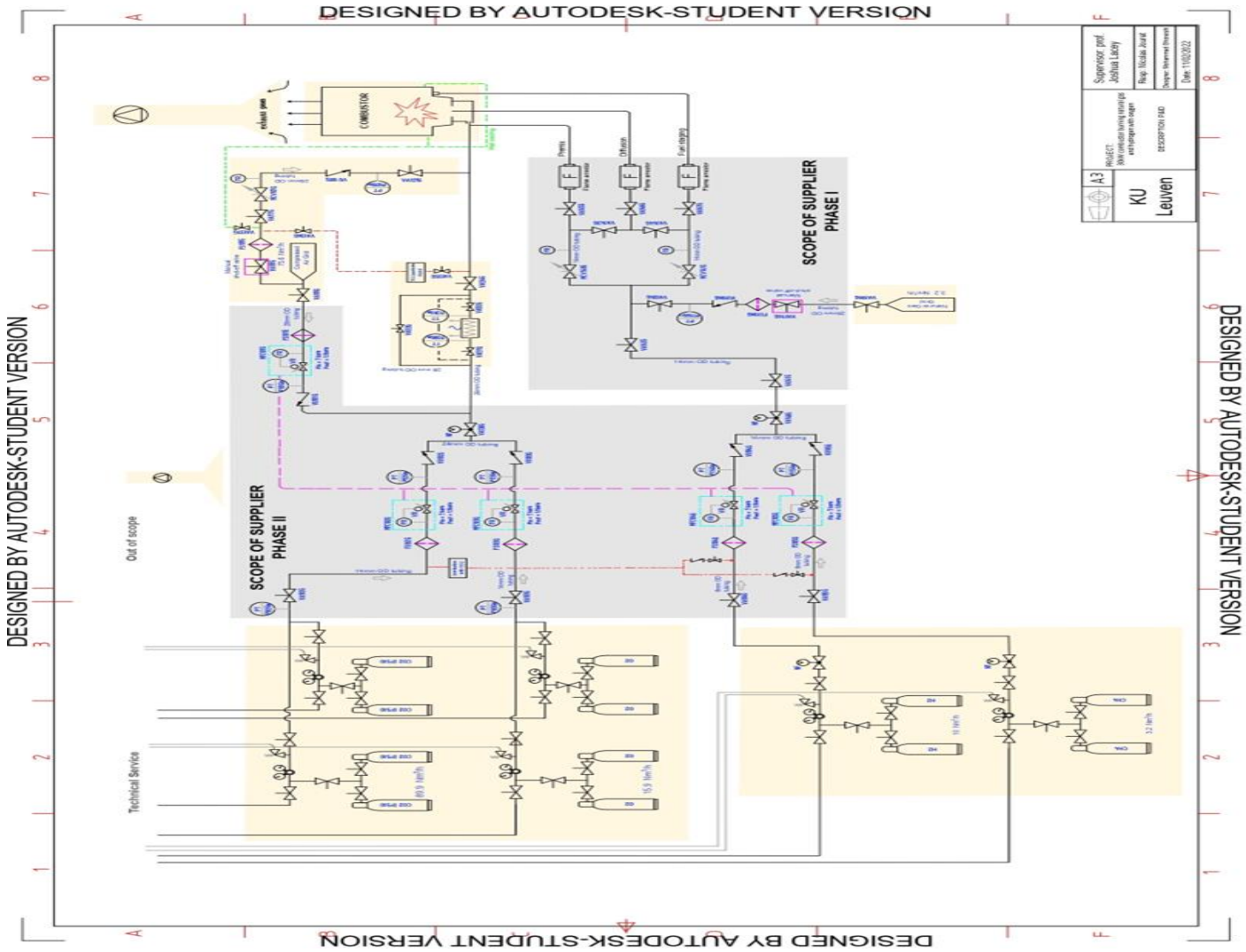

Appendix 4. Process and Instrument Drawing (P&ID) – general scope

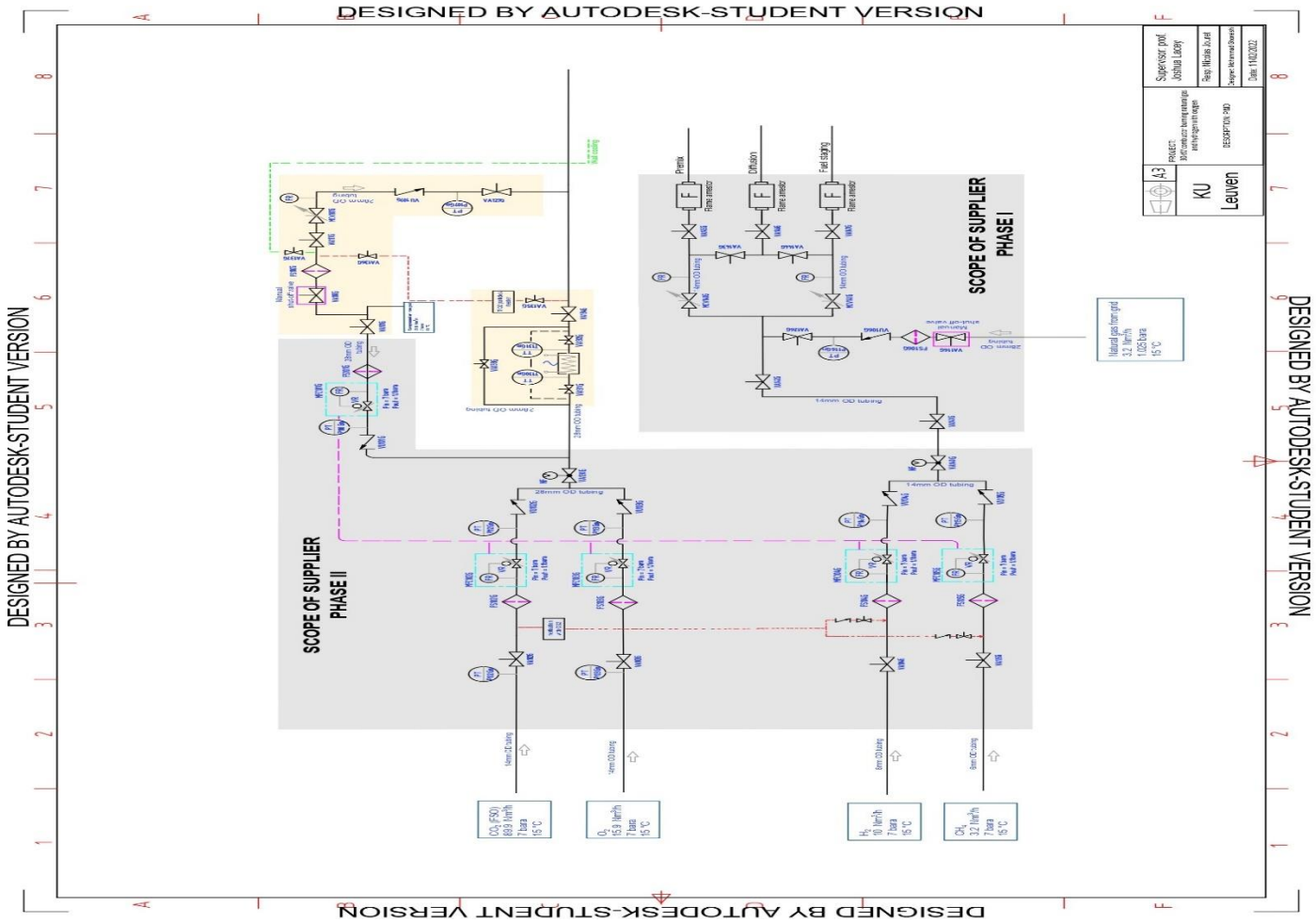

Appendix 5. Process and Instrument Drawing (P&ID) – supplier scope

Base Load			Volumetric Flow Rate		Mass Flow Rate	Density	Output	Mass Flow Rate	Volumetric Flow Rate		
Ch_4	H_2	Lhv	Ch_4	H_2	Kg/H	Kg/Nm^3	Kj/S Or Kw	Kg/H	Total	Ch_4	H_2
mol%	mol%	kJ/mol	Nm^3/h	Nm^3/h					Nm^3/h	Nm^3/h	Nm^3/h
100	0	829.9	3.12	0	2.38	0.75	30.4	2.38	3.12	3.12	0
99	1	824.1	3.09	0.06	2.39	0.75	30.5	2.38	3.14	3.11	0.03
98	2	818.2	3.06	0.06	2.34	0.74	30.0	2.38	3.16	3.10	0.06
95	5	800.6	2.96	0.16	2.28	0.72	29.3	2.36	3.23	3.07	0.16
92.5	7.5	786.0	2.89	0.23	2.23	0.70	28.8	2.35	3.29	3.05	0.25
90	10	771.3	2.81	0.31	2.17	0.69	28.3	2.34	3.36	3.02	0.34
85	15	742.0	2.65	0.47	2.07	0.65	27.2	2.31	3.49	2.97	0.52
80	20	712.7	2.50	0.62	1.96	0.62	26.1	2.28	3.63	2.91	0.73
75	25	683.4	2.34	0.78	1.86	0.59	25.1	2.25	3.79	2.84	0.95
70	30	654.2	2.18	0.94	1.75	0.55	24.0	2.22	3.96	2.77	1.19
60	40	595.6	1.87	1.25	1.54	0.49	21.8	2.14	4.35	2.61	1.74
50	50	537.0	1.56	1.56	1.33	0.42	19.7	2.05	4.82	2.41	2.41
40	60	478.4	1.25	1.87	1.12	0.35	17.5	1.94	5.41	2.17	3.25
30	70	419.8	0.94	2.18	0.90	0.29	15.4	1.79	6.17	1.85	4.32
20	80	361.2	0.62	2.50	0.69	0.22	13.2	1.59	7.17	1.43	5.74
10	90	302.6	0.31	2.81	0.48	0.15	11.1	1.32	8.56	0.86	7.70
0	100	244.0	0	3.12	0.27	0.09	8.9	0.92	10.61	0	10.61

Appendix 6. Hydrogen addition to natural gas in a 30 kW burner and same input heat

Scenario		**A**	**B**	**C**	**D**	**E**	**F**	**G**	**H**	I
CH_4	Nm^3/h	3.2	2.4		3.2	2.4		3.2	2.4	
H_2	Nm^3/h		2.4	10.0		2.4	10.0		2.4	10.0
CH_4 + H_2	Nm^3/h	3.2	4.8	10.0	3.2	4.8	10.0	3.2	4.8	10.0
			Phi = 1.18							
Air	Nm³/h	25.6	24.3	20.2						
O_2	Nm^3/h				5.4	5.1	4.2	5.4	4.2	5.4
CO_2	Nm^3/h				12.6	11.9	9.9	30.5	9.9	30.5
			Phi = 1.0							
Air	Nm^3/h	30.2	28.7	23.8						
O_2	Nm^3/h				6.3	6.0	5.0	6.3	5.0	6.3
CO_2	Nm^3/h				14.8	14.1	11.7	36.0	11.7	36.0
			Phi=0.80							
Air	Nm^3/h	37.8	35.9	29.8						
O_2	Nm^3/h				7.9	7.5	6.3	7.9	6.3	7.9
CO_2	Nm^3/h				18.5	17.6	14.6	45.0	14.6	45.0
			Phi = 0.60							
Air	Nm^3/h	50.4	47.8	39.7						
O_2	Nm^3/h				10.6	10.0	8.3	10.6	8.3	10.6
CO_2	Nm^3/h				24.7	23.4	19.4	60.0	19.4	60.0
			Phi = 0.40							
Air	Nm^3/h	75.6	71.7	59.5						
O_2	Nm^3/h				15.9	15.1	12.5	15.9	12.5	15.9
CO_2	Nm^3/h				37.0	35.1	29.2	89.9	29.2	89.9
CO_2	Nm^3/h				37.0	35.1	29.2	89.9	29.2	89.9

Appendix 7. Fuel and oxidizer flow rate calculation based on the equivalence ratio

Application	**V (m/s)**
Water Pipes	
General	1-3
Main lines	1-2
Ancillary pipes	0.5-0.7
Transport issues	1.5-3
Suction lines of pumps	0.5-1
Pressure pipes of pumps	1.5-3
High-pressure water pipes	15-20
Water turbines	2-6
Air Ducts	
Compressed air lines	2-10
Air (normal condition)	10-40
Gas Pipelines	
High-pressure pipes	5-15
Low-pressure grid, main lines	3-10
Pipes in tube	0.5-1

Appendix 8. Economic flow velocities in pipelines for various media in m/s

References

Akram A., Kumar, M., Paidi, S., Bhavaraju, S. K. (2013) Effect of n2/co2 dilution on the laminar burning velocity of h2-air mixtures at high temperatures, *Int J Hydrogen Energy*, 38(**31**): 13812–13821.

Alousi, Al., Karim, G. A., Wierzba, I. (1996) Methane-hydrogen mixtures as fuels, *International Journal of Hydrogen Energy*, **21**: 625–631.

Andrews, G. E., Bradley, D. (1972) Determination of burning velocities: A critical review, *Combustion and Flame*, **18**: 133-153.

Bian, J., Zhao, Z., Zhang, H., Huang, M., Cai,, Z., Wang, X. (2020) Self-similar propagation, and turbulent burning velocity of ch4/h2/air expanding flames: effect of Lewis number, *Combust Flame*, **212**: 1–12. https://doi.org/10.1016/j.combustflame.2019.10.019.

Bosschaart, L. P. H., deGoey, K. J. (2004) The laminar burning velocity of flames propagating in mixtures of hydrocarbon and air was measured with the heat flux method, *Combust Flame*, 136(**3**): 261–9.

Chigier, N. A. Beer, J. M. (1972) Combustion aerodynamics, Applied Science Publishers, London, pp: 106.

Clague, T., Pilling, A. R., Hughes, M. J., Turanyi, K. J., (2001) Development and testing of a comprehensive chemical mechanism for the oxidation of methane, *International Journal of Chemical Kinetics*, **33**: 513–538.

Coumans, S. C., Slikker, K., de Andrade Oliveira, W. J., Bastiaans, M. H., Goswami, R. J., Derks, M. (2013) The effect of elevated pressures on the laminar burning velocity of methane + air mixtures, *Combust Flame*, 160(**9**): 1627–35.

D'Alessio, J., Moccia, V. (2013) Burning behaviour of high-pressure ch4-h2-air mixtures, CNR Motors Institute.

Dahoe, L. P. H., de Goey, A. E. (2003) On the determination of the laminar burning velocity from closed vessel gas explosions, *J. Loss Prev. Process Ind*., 16(**6**): 457–478.

Dincer, 'II Rosen, M. A., Midilli, A., Ay, M. (2005) On hydrogen and hydrogen energy strategies: I: current status and needs, *Renewable and Sustainable Energy Reviews*, 9(**3**): 255-271.

Driscoll, J. F., Hsieh, A., Dahm, W. J. A. (1998) Scaling laws for nox emission performance of burners and furnaces from 30 kW to 12 MW, *Combustion and Flame*, **114**: 54–80.

Dryer, F. L. Westbrook, C. K. (1984) Chemical kinetic modeling of hydrocarbon combustion, prog. energy combust, *Int. J. Press. Vessel. Pip.*, doi: 10.1016/ 0360-1285(84)90118-7., **10**: 1–57.

Duan, X.; Li, Y.; Liu, Y.; Zhang, S.; Guan, J., L, M. C. (2020) Dilution gas and hydrogen enrichment on the laminar flame speed and flame structure of the methane/air mixture, *Fuel*, **281**: 118794.

Dumitras, G., Charon, O. Horbaniuc, B., Marin, O. (2004) Oxygen-enriched combustion in supercritical steam boilers, *Energy*, **29**: 427–448.

El Hefni, B., Bouskela, D. (2019) Combustion Chamber Modeling, Modeling and Simulation of Thermal Power Plants with Thermo Sys Pro: A Theoretical Introduction and a Practical Guide, pp: 165-185.

Exhaust gases from combustion and industrial processes, (1971) EPA contract no. ehsd 71-36, washington, dc. Engineering Science, In-corporated., October 1971.

F Gas pipeline hydraulics (2005) Menon, E. S., CRC Press.

Forster, D., Kneer, M., Heil, R., Toporov, P. (2011) Experimental investigation on the effect of O_2 and CO_2 on burning rates during oxyfuel combustion of methane, *Proc Combust Inst*., 33(**2**): 3407–13.

Frenklach, D., Moriarty, M., Eiteneer, N., Goldenberg, B., Bowman, M., Hanson, C., Song, R., Lissianski, S., Jr., W. G., Smith, V., Golden, G., Qin, Z. (1999) GRI-mech homepage, Gas Research Institute.

Glarborg, L. L. B., Bentzen, P. (2007) Chemical effects of a high CO_2 concentration in oxy-fuel combustion of methane, *Energy Fuels*, 22(**1**): 291–6.

Gollahalli, S. R., Choudhuri, A. R. (2003) Characteristics of hydrogen–hydrocarbon composite fuel turbulent jet flames, *International Journal of Energy Research*, **28**: 445–454.

Golomb, D., Herzog, H. (2004) Carbon capture and storage from fossil fuel use, Encyclopedia of Energy, Cambridge, MA: *Massachusetts Institute of Technology*, **1**: 1–11.

Hagiwara, A., Bortz, S. (1984) Studies on the near field aerodynamics of swirl burners; results of the NFA 1 investigation, Flow visualization and hot wire measurements in isothermal swirling flows, Netherlands: N. p., 1984, Web.

Hals, J. Ditaranto, M. (2006) Combustion instabilities in sudden expansion of oxy-fuel flames, **146**: 439–512.

Halter, F., Foucher, F., Landry, L., Mounaïm-Rousselle, C. (2009) Effect of Dilution by Nitrogen and/or Carbon Dioxide on Me-thane and Iso-Octane Air Flames, *Combustion Science and Technology*, 181(**6**): 813-827. DOI: 10.1080/00102200902864662.

Hermanns, R. T. (2007) Laminar burning velocities of methane-hydrogen-air mixtures.

Hord, J. (1978) Source book for hydrogen applications, hydrogen research institute and national renewable energy laboratory, *International Journal of Hydrogen Energy*, **3**: 157–176.

https://p.cygnus.cc.kuleuven.be/bbcswebdav/pid-31437329-dt-content-rid-3101464183/orgs/c130038-b-2122/rm%20tabel%20leidingsverliezen.pdf

Hu, E., Jiang, X., Huang, Z., Iida, N. (2012) Numerical study on the effects of diluents on the laminar burning velocity of the methane-air mixtures, *Energy Fuels*, 26(**7**): 4242-52.

Ilbas, M., Crayford, A. P., Yılmaz, I., Bowen, P. J., Syred, N. (2006) Laminar-burning velocities of hydrogen–air and hydrogen–methane–air mixtures: An experimental study, *International Journal of Hydrogen Energy*, 31(**12**): 1768-1779.

International Energy Agency (2018) world energy outlook, https://www. iea.org/weo2018/scenarios/.

International Organization for Standardization (ISO) (1995) Natural gas, calculation of caloric values, density, relative density and wobbe index from composition, December, 1995.

Jouret, N. (2021) Safety aspects of thermal systems, chapter 3: Boiler (firing), ku leuven.

Ju, N., Kohse-Hoinghaus, Y., Law, K., Qi, C. K., Egolfopoulos, F., Hansen, F. N. (2014) Advances and challenges in laminar flame experiments and implications for combustion chemistry, *Progr Energy Combust Sci*., 43:36–67.

Karim, G. A. (1987) The dual fuel engine. In: Evans RL, editor. Automotive engine alternatives, New York: Plenum Press.

Kelley, C. K., Law, A. P. (2009) Nonlinear effects in the extraction of laminar flame speeds from expanding spherical flames, *Combust Flame*, 156(**9**): 1844–1851.

Kharel, B., Shabani, S. (2018) Hydrogen is a long-term large-scale energy storage solution to support renewables, *Energies*, **11**: 2825.

Kiga, T., Takano, S. Shikisima, S., Kimura, K., Omata, K. (1995) The characteristics of pulverized coal combustion in O_2/CO_2 mixtures for CO_2 recovery, *Energy Convers*, (**36**): 805–8.

Kim, N. I., Kim, G. T., (2011) Laminar burning velocity predictions by mesoscale flames in an annular diverging tube, *Fuel*, 90(**6**): 2217–23.

Lawes, M. Z., Woolley, M., Gu,, R., Haq, X. J. (2000) Laminar burning velocity and market in lengths of methane-air mixtures, https://doi.org/10.1016/s0010-2180(99)00142-x, *Combust Flame*, 121(**1-2**): 41–58.

Majkut, M., Stolecka, K., Witkowski, A., Rusin, A. (2018) Analysis of compression and transport of the methane/hydrogen mixture in existing natural gas pipelines, *Int. J. Press. Vessel. Pip*, **166**: 24– 34.

Mehra, R. K., Huang, Z., Luo, S., Ma, F. (2020) Deep insights of hcng engine research in China, *Fuel*, **263**: 116612–116629.

Metcalfe-W, A., Curran, K., Davis, H. J., Mathieu, O., Donohoe, M. L., Heufer, N. (2013) Ignition delay times, laminar flame speeds, and mechanism validation for natural gas/hydrogen blends at elevated pressures, https://doi.org/10.1016/j.combustflame, *Combust Flame*, 161(**6**): 1432–1443.

Milton, J. C., Keck, B. E. (1984) Laminar burning velocities in stoichiometric hydrogen and hydrogen hydrocarbon gas mixtures, *Combust Flame*, 58(**1**): 13–22. https://doi.org/10.1016/0010-2180 (84)90074-9.

Miyake, J. (1997) Explosion characteristics and safety evaluation of hydrogen, Hydrogen Energy Systems Society, Japan, **2**: 9–17.

Mortimer, N. (2009) What are the life cycle analysis and socio-economic issues (final presentation) identify the issues related to using hydrogen as primary energy source: Emissions, employment, and cost, lough borough university, UK.

Mulligan, N., Hoekstra, R. L., Collier, K. (1994) Demonstration of hydrogen mixed gas vehicles, *International Journal of Hydrogen Energy*, 3: 1781–1796.

Ogami, H., Kobayashi, Y. (2005) Laminar burning velocity of stoichiometric ch4/air premixed flames at high pressure and high temperature, *JSME Int. J. Series B. Fluids Thermal Eng*., 43(**8**): 603–609.

Oh, D., Noh, J. (2012) Laminar burning velocity of oxy-methane flames in atmospheric condition, *Energy*, **45**: 669–675.

Ouimette, P., Seers, P. (2009) Numerical comparison of the premixed laminar flame velocity of methane and wood syngas, *Fuel*, 88(**3**): 528–33.

Palmer, A. D., Croiset, E., Thambimithu, K. V. (1999) A novel strategy for greenhouse gas abatement in a coal-fired power plant, proceedings of the combustion Canada 99 conference, Calgary, Canada.

Penev, M., Melaina, M. W, Sozinova, O. (2013) Blending hydrogen into natural gas pipeline networks: A review of key issues, United States, *Fuel*, 1: 17–34.

Perry, J. H. (1963) Chemical engineers' handbook, fourth edition, McGraw-Hill Book Company, New York, NY.

Petersen, E., Bourque, O., Curran, G., Plichta, H., Mathieu, D. (2013) Laminar flame speeds of natural gas blends with hydrogen at elevated pressures and temperatures, 8th U.S. National Combustion Meeting.

Plasynski, S., McIlvried, H., Srivastava, R. D., Figueroa, J. D., Fout, T. (2008) Advances in CO_2 capture technology, US department of Energy's carbon sequestration program, *International Journal of Greenhouse Gas Contro*l, **2**: 9–20.

Qin, Y., Ju, X., (2005) Measurements of burning velocities of dimethyl ether and air-premixed flames at elevated pressures, *Proc Combust Inst*, 30(**1**): 233–40.

Rallis, C. J., Garforth, A. M. (1980) The determination of laminar burning velocity, *Prog. Energy Combustion. Sci*, **7**: 302-329.

Razus, V., Oancea, D., Mitu, D., Giurcan, M. (2017) Inert gas influence on the laminar burning velocity of methane-air mixtures, *J Hazard Mater,* **321**: 440–8.

Rosseel, E., Sierens, R. (2000) Variable composition hydrogen/natural gas mixtures for increased engine efficiency and decreased emissions, *Journal Engineering Gas Turbines Powe*r, **122**: 135–140.

Scheitrum, D. McDonald, Z., Miller, M. Ogden, J., Jaffe, A. M. (2018) Natural gas as a bridge to hydrogen transportation fuel: Insights from the literature, energy policy, *Int. J. Press. Vessel. Pip*, **115**: 317–329.

Smooke, Mitchell, D. (2013) The computation of laminar flames', proceedings of the combustion institute, *International Journal of Hydrogen Energy*, 34(**1**): 65-98.

Stolaroff, J. K., Keith, D. W., Ha-Duong, M. (2006) Carbon capture and storage from fossil fuel use, Climatic Change, *Springer Verlag*, **74**: 17–45.

Thambimithu, K. V. Croiset, E. (1998) Coal combustion with flue gas recirculation for CO_2 recovery, proceedings of the fourth international conference on greenhouse gas control technologies, Interlaken, Switzerland, pp: 581.

Uehara, I. (2011) Hydrogen and natural gas mixture. National Institute of Advanced Industrial Science and Technology, Japan, **3**: 1781–1796.

Vanoverberghe, V. (1992) Flow, turbulence and combustion of premixed swirling jet flames, KULeuven, January, 2004.

Weber, R. Dugue, J. (1992) Burner specifications: Design and calibration of a 30 kW natural gas burner, Technical Report Doc, Netherlands.

Williams, F., Joseph, A., Grcar, F. (2009) A hypothetical burning-velocity formula for very lean hydrogen–air mixtures, Proceedings of the Combustion Institute, 32(**1**): 1351-1357.

Wu, C. K., Law, C. K. (1985) On the determination of laminar flame speeds from stretched flames, *Symp (Int) Combust*, 20(**1**): 1941–9.

Wu, C. K., Yu, C. K., Law, G. (1986) Laminar flame speeds of hydrocarbon + air mixtures with hydrogen addition, *Combust Flame*, pp; 339–347.

Wu, M. S. Driscoll, J. F., Dahm, W. J. A. (1993) Scaling characteristics of the aerodynamics and low-nox properties of industrial natural gas burners: The 30kw test results, united states: The scaling 400 study, part 3.

Yu, E. S., Cha, J. M., Lee, T., Kim, J., Mun, D. (1996) National fire protection association incorporated, code 30, chapter 2, page 18, section 3.7.3, 1996 edition, quincy, ma.

Zhang, J. H., Gong, M., Jin, J., Huang, W., Xie, Z. H., Wang, Y. L. (2013) Experimental and numerical study on laminar flame characteristics of methane oxy-fuel mixtures highly diluted with CO_2, *Energy Fuel*, 27(**10**): 6231–7.

Ziębik, A., Liszka, M. (2010) Coal-fired oxy-fuel power unit e process and system analysis, *Energy*, **35**: 943– 51.